Refined Predictions Compared with the Propulsion Airframe Aeroacoustics and Aircraft System Noise Flight Research Test Data

Russell H. Thomas, Yueping Guo, Eric H. Nesbitt, Ian A. Clark and Jason C. June

NASA Langley Research Center, Hampton, VA 23681, USA

Abstract

In a collaboration between NASA and The Boeing Company, the Propulsion Airframe Aeroacoustics and Aircraft System Noise Flight Research Test was executed by the Boeing ecoDemonstrator Program in 2020 with an Etihad Airways Boeing 787-10 aircraft. This ambitious flight research successfully accomplished many objectives and constitutes the most comprehensive and highest quality acoustic flight data available to NASA for a modern commercial subsonic transport aircraft. One purpose of these data is to be the measure of accuracy for the aircraft system noise prediction capabilities of NASA. This research reviews the impact of the major improvements in prediction methods implemented up to this point and tested in the Research version of the NASA Aircraft Noise Prediction Program. The improvements have been to the prediction of jet source and jet-flap interaction, to both fan broadband and tone source prediction, and to the prediction of propulsion airframe aeroacoustic scattering effects. In general, over the engine power range, comparisons between prediction and flight data are within 2 EPNdB including for the intentional sideline-to-sideline asymmetries as implemented in the flight test by flying the aircraft with only one engine at power. Considerable progress has been shown here in the continuing effort to advance the fidelity of NASA aircraft noise prediction capabilities for subsonic aircraft flight acoustics, modern transport aircraft and future aircraft concepts.

Keywords: aircraft noise prediction, flight acoustics.

1. Introduction

The NASA Aeronautics Research Mission Directorate continues to work to improve the capabilities and the fidelity of aircraft system noise prediction through sustained internal research and a wide range of partnerships. The fundamental driving motivation is the necessity for the air transport system to be compatible with quality of life for the populations impacted by aviation noise every day. The applications relevant to the sponsor of this research, the Advanced Air Transport Technology Project, range from current subsonic commercial aircraft to future advanced aircraft concepts and technologies [1]–[10]. Capabilities have been developed through a broad spectrum of theoretical, computational, experimental, and validation efforts [11]–[13]. Despite these extensive and long-term efforts, acoustic flight data on a relevant modern commercial subsonic transport have been lacking due to the many obstacles for an endeavor of this large scale and scope. However, full-scale, high-quality flight data are critical to many aspects of the NASA aircraft noise capabilities. This type of information is critical to performing rigorous assessment of the current state of the NASA internal research level aircraft system noise tool, the Aircraft NOise Prediction Program (ANOPP-Research). ANOPP-Research is different from the released version of ANOPP in that ANOPP-Research has the newest methods under development and testing. Flight data are also essential to enable future improvements in prediction capabilities and to develop increasingly advanced noise reduction technologies and approaches. Therefore, to address this long-standing and critical gap, the NASA

Advanced Air Transport Technology (AATT) Project funded an ambitious acoustic flight research effort, the Propulsion Airframe Aeroacoustics and Aircraft System Noise (PAA & ASN) Flight Research Test in 2020.

Propulsion Airframe Aeroacoustic (PAA) effects are the interactions from integration of the propulsion and airframe and include both the acoustic and flow interactions. PAA flow interaction effects can often have significant directivity and magnitude effects such as from inflow distortion, jet-pylon, or jet-flap interactions. Shielding, reflection, and diffraction are acoustic scattering interactions and are a function of how the aircraft configuration integrates the propulsion system with the airframe. Acoustic scattering is influenced by flowfield direction and shear layer characteristics. Acoustic scattering is significantly influenced by the characteristics of the engine noise sources including spectral content, distribution, and directivity. Airframe edge geometry details, control surfaces, and flight parameters can also influence the magnitude and directivity of the PAA effects. A useful, initial classification of PAA effects was made in Thomas et al. [1] based on this approach and has been an effective framework.

Aircraft system noise is defined as the sum of all contributing noise elements including noise sources, PAA interactions, and airframe-to-airframe interactions (e.g., gear wake interacting with a high-lift flap).

Realistic features that can impact the noise of all the aircraft sources, flight effects, and all types of PAA effects are physical and integral aspects of aircraft system noise. Understanding and predicting all of these is essential to the pursuit of higher fidelity, more realistic, and more accurate predictions of system noise. This is equally true for today's aircraft as well as for future, unconventional aircraft, and even more so for low noise aircraft. An additional requirement is the need for a total cycle time (setup, running, and post analysis) that supports the design process of industry. The research in this paper addresses this goal directly.

2. Summary of this Research Series

This paper is part of a series of papers that are all related to the NASA/Boeing PAA & ASN Flight Research Test covering the planning, execution, analysis of results, and the development of new prediction methods.

At the 28th AIAA/CEAS Aeroacoustics Conference in June 2022, a NASA overview paper [14] described the motivations, objectives, and predictions that contributed to the detailed flight test design. The NASA overview paper was accompanied by a Boeing-led overview paper [15] that focused on the flight test execution, the design of the extensive instrumentation package required to produce the high-quality data, the test procedures, and some key results from the community noise microphone measurements. These two papers together provide a complete overview of the comprehensive research designed into this flight test.

A photograph of the flight test site with the aircraft executing a banking maneuver test condition over the ground instrumentation is shown in Fig. 1. The location of the ground phased microphone array's location is shown in the photograph. This array was comprised of a total of 954 microphones and was used for noise source localization. In addition, there is a centerline linear array as well as south and north (not pictured) sideline microphone arrays, which are symmetric about the centerline.

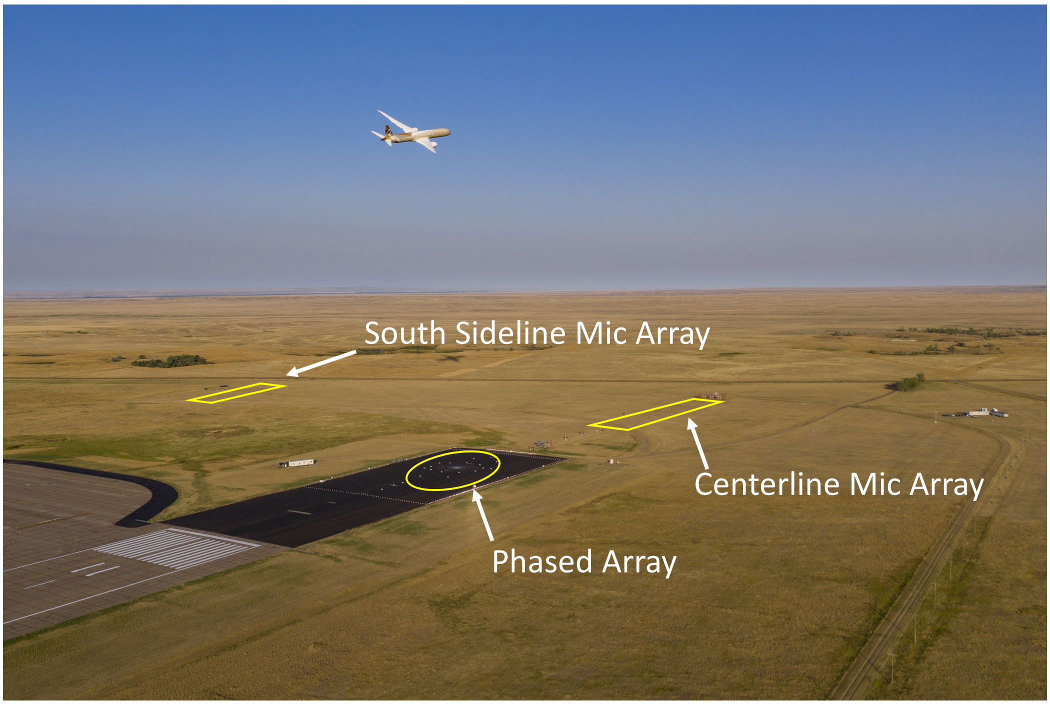

Figure 1 - Test site near Glasgow, Montana, with the Etihad Airways 787-10 aircraft banking over the ground instrumentation. Only the South Sideline, Centerline, and Phased Array are identified. The North Sideline microphone array is located just to the right of the photo boundary [Photo Credit: The Boeing Company].

Figure 2 shows another aspect of the design of the flight test, the result of combining the NASA technical approach and prediction work and the Boeing experience and instrumentation expertise to add on-aircraft instrumentation. The challenge was to measure PAA effects from instrumentation on the aircraft itself. A total of 216 microphones were installed on the surface of the aircraft, and the instrumentation was arranged in four arrays, once again enabling the accomplishment of multiple objectives. The four arrays are the axial array (along the fuselage length), the circumferential array (forward of the wing), the over-wing array, and the under-wing array.

The purpose of the axial array, combined with the over-wing array, was to measure all three regions of fan-radiated noise, namely the direct field, the diffracted and transition regions from the leading and trailing edges, and the shielded (shadow) region directly above the wing. These arrays should measure the full distribution of forward-radiated and aft-radiated fan noise as scattered by the wing. Engine power and high-lift deflection could also augment this study with additional parameters that can impact the scattering.

The circumferential array is forward of the wing to measure the forward fan-radiated sound field. This can provide a measure of the peak radiation angle of inlet fan noise as well as general directivity. However, by making the array around the circumference, this array can also measure the incidence field for the diffraction around the fuselage and to the far field. This created the possibility of a shielding experiment to the far field and will be discussed below.

The under-wing array is intended to measure the direct field of the engine providing source definition of the aft fan and jet sources. These measurements will be used as input to the shielding attenuation determination from the other arrays above the wing. Finally, the under-wing array may provide some quantification of the reflected level and primary reflection locations.

The analysis of these results will be covered in future work.

Figure 2 - Test aircraft outfitted with fuselage mounted microphones in four arrays: Over-wing, Under-wing, Axial, and Circumferential. Additional photos and details in Czech et al. [15]. [Photo Credit: The Boeing Company].

In addition to the two overview papers from 2022, additional papers addressed detailed analyses approaches and results for topics of airframe noise sources and the flight effects of fan noise [16], [17]. The comparison of airframe source predictions from ANOPP-Research with the flight test data showed excellent agreement and was an initial successful validation of the improved third-generation of system level airframe source noise methods. The NASA overview paper also showed aircraft system level predictions compared to the community noise microphone data. This result showed that there was much needed improvement in the prediction accuracy. Considering the results across the set of papers, there was need for prediction improvements notably in fan source noise, liner attenuation, trailing edge source noise, flap source noise, and several additional PAA effects such as flow effects on scattering, jet-flap interaction, and others. This overall result was suspected for a long time and served as one of the powerful motivations for this flight test.

3. Aircraft System Level Prediction

3.1 ANOPP

In 1973, a focused aircraft system noise prediction activity was established at the NASA Langley Research Center. The mission was to develop a state-of-the-art method for predicting aircraft noise for a range of aircraft types from in-service aircraft to future concept aircraft. As described by Raney et al. [18], there were two major goals. The first was to predict effective perceived noise level (EPNL) to within ±1.5 dB, a value related to the 90% confidence interval from the noise regulation and, therefore, still relevant today. The second was to establish the relationships of noise to the design and operation of aircraft in order that aircraft noise constraints could be incorporated into the preliminary design process. This second goal also is completely relevant to the present and perhaps more so as the scope of aircraft technologies continues to expand.

This effort resulted in the creation of the NASA Aircraft NOise Prediction Program (ANOPP). The theoretical foundation of the ANOPP prediction process is described in the original publication [19]. Sustained development has continued since that time with a constantly evolving scope of the aircraft concept types and technologies to consider.

Over the past five decades, all aspects of aircraft noise research, including measurement technology, computing power, understanding of acoustic physics, and aircraft design and technology, have undergone significant changes. Nevertheless, it remains a grand challenge to develop robust, accurate, physics-based prediction methods to meet the most stringent requirements of aircraft system noise and to develop efficient noise reduction technologies. These most stringent requirements are for accuracy, a total turnaround time (not including the initial setup process) on the order of a less than a day to be useable in design and optimization cycles, and with sufficiently resolved parameters and results to be useful to provide design guidance.

3.2 ANOPP-Research

From the beginning of ANOPP, there was a recognition of the need for and an emphasis on the development of new prediction methods in efforts to improve the accuracy of prediction and to extend prediction capabilities as technology advanced over the decades. In addition, beginning in the 2000s, ANOPP2 was created with the goals of providing a modern programming structure with greater efficiency, flexibility, and more capabilities [20].

For the past two decades, both ANOPP and ANOPP2 have continued to be developed in coordination. Best practice at NASA for predicting a fixed wing aircraft is to use ANOPP together with ANOPP2 to take advantage of user interfaces, utilities, and efficiency of ANOPP2 while all the methods for noise sources are still a part of ANOPP.

The improved prediction capabilities are needed to improve accuracy and address the challenges presented by changing technologies of modern and future subsonic transport aircraft and new noise reduction opportunities. In addition, achieving future anticipated system level metrics requires advanced aircraft concepts and technologies that create additional prediction challenges. Low pressure ratio fan noise, unducted propulsors, duct liner attenuation, core noise, airframe noise, and PAA effects all represent much needed improved prediction methods for the NASA aircraft system noise capability. In addition, these improvements ideally should be more physics-based to include details of the full fidelity aircraft system while having a fast total turnaround time to enable a more direct linkage to preliminary design and optimization.

In recent years, ANOPP-Research has been a NASA internal version of ANOPP that is differentiated from the ANOPP version that is released to US users. The purpose of ANOPP-Research has been to deploy the best capabilities available for NASA system noise studies and to gain experience with new methods under development. ANOPP-Research utilizes unique experimental information, prediction and experimental experience, and new research-level prediction methods. ANOPP-Research has been used extensively in the past decade on many NASA system noise studies [1]–[10]. An overview of the prediction process and the elements of ANOPP-Research as of 2022 are given in Thomas et al. [14]. As part of this continuing effort, there has been significant progress in the development of several new methods in ANOPP-Research which is described in the following section.

4. ANOPP-Research Prediction Improvements

The initial comparison of measured total aircraft noise with predictions was described in Refs. [14], [16], and [17]. Together, the three provided a good overall initial assessment of the status of ANOPP-Research as of 2022. These predictions used the best capabilities in ANOPP-Research that have been utilized in system noise studies by NASA in recent years and that were most applicable to a prediction of the 787-10.

The major focus of the current research in the present paper is to accumulate the key improvements that have been made since 2022 in the ANOPP-Research prediction process and to compare with the flight test data in order to investigate continued improvement in accuracy relative to the flight test data. The improvements will be in several areas of prediction including more accurate accounting of liner areas, fan source noise, jet source noise, and improvements in the prediction of several PAA effects for both jet and fan broadband noise.

4.1 More Accurate Aft and Inlet Liner Areas

For duct liner attenuation, the method of Kontos et al. [21], referred to as the TREAT method in ANOPP, continues to be used but with the 10% area correction factor used in previous studies as a way to account for the added effectiveness of current spliceless liner technology when applied to the inlet broadband fan noise.

The improvement for the current predictions is the result of more accurate accounting of the dimensions of the lined area in both the aft duct and the inlet. For the aft duct, the resulting changes to the input dimensions for TREAT have the effect of lowering the peak frequency of the attenuation spectrum.

For the inlet, dimensions are added to account for the fan case treatment, which was not accounted for in the 2022 predictions. The result of the change increases the overall effectiveness of the inlet liner but does not change the peak frequency of the attenuation spectrum.

4.2 Proposed Fan Source Noise Model

The fan source noise model of Krejsa and Stone [22] has been the best method used in NASA system noise studies for the past decade, with the exception of cases where data were available to use in a data-based method. Nevertheless, there have been results that indicate discrepancies in comparisons with wind tunnel data for geared fans [4]. More significantly, with the initial comparisons to the PAA & ASN 787 flight test data, Clark et al. [17] showed discrepancies particularly in the aft arc.

As a result, there has been a long recognized need for an improved prediction capability for fan source noise. The work of Clark et al. [17] indicated several opportunities for improvement. Using data from both this flight test and the Quiet Technology Demonstrator 2 flight test [23] a proposed new fan source noise prediction method has been developed and reported in Clark et al. [24] for aft fan broadband noise. In a companion paper, Nesbitt et al. [25] also proposes a new model for both inlet and aft-radiated fan tones drawing on the same two flight tests. The proposed models exhibit improved performance with respect to directivity and spectral content, and they utilize a more physical dependence on fan operating condition compared with the method of Krejsa and Stone [22].

While the new methods show great improvement, they are termed proposed models as there is additional work to finalize before more general application. Use in the current work is consistent with the ANOPP-Research process of deploying the best available methods.

4.3 Jet Source and PAA Effects

For the 2022 study, the jet source noise was predicted by the method of Stone et al. [26], while the prediction of the jet PAA effects used the method based on experimental data from the NASA/Boeing PAA series of experiments performed in the Boeing Low Speed Aeroacoustics Facility (LSAF) [27]–[32]. This approach has been considered the best method available to NASA and used in ANOPP-Research predictions for more than a decade. For the 787-10, the following jet PAA effects were included:

- Reflections of the jet noise from the wing, flap, and fuselage together with PAA flow interactions including jet-pylon, jet-flap, and wing downwash. These effects were predicted using data with a 777 airframe and representative separate flow nozzle with pylon but without chevrons.

- The angle-of-attack effect on the jet is predicted using a NASA model also based on data from the NASA/Boeing PAA series of experiments.

The current data-based prediction draws from the same NASA/Boeing PAA series of experiments, this time for prediction of both the jet source including pylon effect, and the jet-flap interaction to make a total prediction of jet source and PAA effects for the 787-10. An improvement over the prediction of 2022 is that now the jet PAA effects are developed from a different subset of the experimental data that includes a chevron nozzle that is representative of the effects of the 787-10 chevron nozzle.

The model scale experimental jet noise, including the interaction of the pylon, was scaled on frequency and level to the 787-10 scale. To account for the significant cycle differences, the acoustic Mach number of the mixed jet was used to interpolate the model scale data to the full scale conditions. In addition, an empirical velocity ratio correction similar to what Viswanathan et al. [33] proposed, was used to account for the differences in the flight effects associated with the different cycle.

The jet-flap interaction noise was derived based on a difference in noise with the addition of the wing, compared to the noise of the jet and pylon, and then scaled to the 787-10 based on the secondary jet velocity ratio. This process resulted in a jet-flap interaction component that included jet scattering from the wing forward of the 90-degree emission angle which, therefore, could not be reliably separated from the jet-flap interaction component. Although jet scattering scales differently than the jet-flap interaction, the expected influence of this effect on total predicted levels is small.

Based on a variety of experiences, the current prediction is expected to show improvements (that is, capturing the physical effects present in the 787-10 flight test with higher fidelity) in the total prediction for both the jet source noise prediction and in several of the jet PAA effects. Left to future work, this prediction will be further improved by separating the forward jet scattering from the jet-flap interaction effect and applying this, along with the scattering from the wing and fuselage aft of the 90-degree emission angle, to the jet mixing noise component.

4.4 Fan Broadband Scattering PAA Effects

In the 2022 study, the prediction of the fan PAA scattering effects included the reflection of fan inlet noise from the fuselage and the reflection of fan exhaust noise from the wing, flap, and fuselage. These effects were predicted with the LSAF-PAA-data-based approach where experimental data [27]-[29] from a broadband source in a nacelle and 777-airframe model were scaled to 787-10 full scale.

As part of developing new capabilities for ANOPP-Research, new physics-based shielding and scattering prediction methods have been created. The Propulsion Airframe Aeroacoustics Shielding Attenuation (PAAShA) method for shielding prediction has been systematically validated [34]. Adding to the shielding methodology in PAAShA, the more general and capable Propulsion Airframe Aeroacoustics Scattering (PAASc) method focuses on the theoretical development of a new system level, midfidelity method to directly predict PAA effects from acoustic scattering [35] including shielding, diffraction, and reflection. This newly developed prediction method was crucial in the design of this flight test. Additionally, this method will be used in the continuing analysis work with the flight test data to study the many aspects of the PAA effects with this aircraft configuration.

In the current study, for the prediction of the scattering effects of fan broadband noise for both inlet and aft-radiated directions, the LSAF-PAA-data-based approach is replaced with a prediction using the PAASc method. This will be a more extensive use of PAASc predictions as compared to the prior validations and includes, for the first time, the use of PAASc-predicted PAA scattering effects in the system noise calculation and presentation of spectra and EPNdB.

The PAASc prediction process requires the airframe geometry and a hemisphere of far field observer microphones. Only a surface grid is needed from the airframe geometry and the far field hemisphere can have any resolution required. The modeling of the noise source is another key element. In this case, fan inlet-radiated broadband noise and fan exhaust broadband noise are the two sources and are modeled separately. Point sources are distributed over the plane of the inlet with the directivity of the fan forward radiated inlet noise supplied by the fan source noise method. A second set of point sources is distributed in the exit plane of the fan bypass duct nozzle and again, the directivity of fan aft-radiated broadband noise is supplied by the aft fan source noise method. The scattering prediction proceeds frequency by frequency to calculate the entire spectrum and propagate to any far field observer with any metric computed.

For this prediction of the 787-10 straight flyover, Figure 3 shows a projection of a hemisphere (below the aircraft) of the scattered field from the inlet-radiated fan noise at the single frequency of 1000 Hz and in terms of a sound pressure level (SPL) difference between an isolated noise source and the noise source with airframe. The prediction shows the expected features of the scattered field given that one engine is at high power and the other at flight idle. There is mostly reflection and concentrated on the same side as the engine at high power and more in the aft angles. Scattering from the curved fuselage is on the order of 1 dB in the region forward of the inlet plane.

Figure 4 shows the scattered field from the aft-radiated fan broadband noise source at 1000 Hz. The location of the aft-radiated noise is directly under the leading edge of the wing. As a result, the scattered field has larger amplitudes and covers a much larger extent of the hemisphere. One area has amplitudes of 5 dB or more. This area, in red in the figure, is attributed to reflection of noise first emitted near peak directivity angles but then reflected by the complex geometry of the airframe to further aft angles where the isolated source directivity decreases. These higher reflected amplitudes do not contribute much to the absolute noise levels because the level of the source (fan broadband in this case) drops off considerably at these high aft angles.

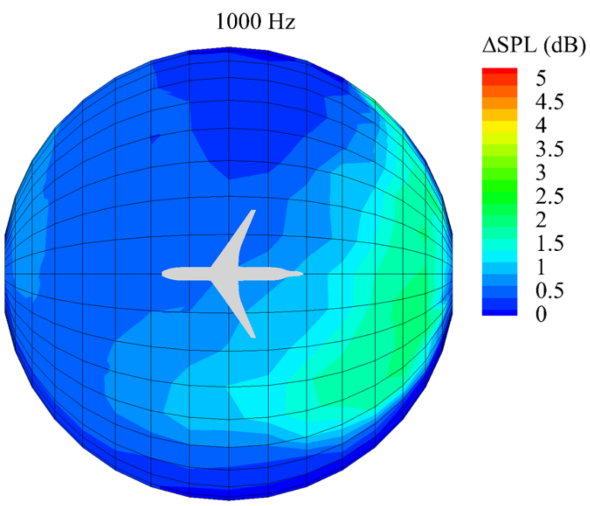

Figure 3 – PAASc-predicted scattered field of inlet-radiated fan broadband noise from the location of the inlet plane on the left (lower) wing.

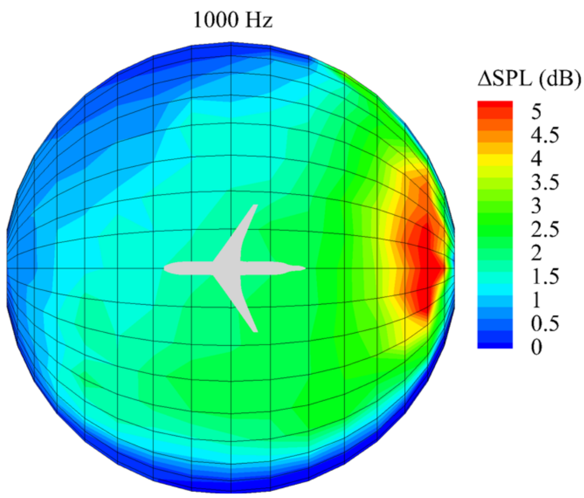

Figure 4 – PAASc-predicted scattered field of aft-radiated fan broadband noise from the location of the bypass duct exit plane on the left (lower) wing.

Figure 5 shows the combined PAASc prediction of scattering for both inlet and aft fan broadband noise at 1000 Hz for this condition with one engine at full power and the other at flight idle. This requires the relative amplitude of the inlet and aft-radiated noise to be adjusted in the PAASc prediction with the predicted levels supplied from the fan source noise method. Of course, the system level prediction requires all frequencies to be calculated by PAASc; 1000 Hz is shown here as an example.

Figure 6 shows, at the same 1000 Hz, the scattered field from the LSAF PAA experiments obtained, by placing a broadband noise source into a nacelle which is positioned at the correct location under the wing of a Boeing 777 airframe. The wind tunnel data include forward flight effect, flap deflection, and other relevant details. In contrast, the current PAASc prediction uses a generic airframe that does not have the geometric details of the 777-airframe wind tunnel model. That is one key difference between the two results and, in general, they are not an equivalent comparison. The PAASc prediction is modeling the predicted full-scale fan noise source rather than the wind tunnel broadband noise simulator. Another difference is that the wind tunnel microphones had an aft angle limit and, as a result, for the prediction, a roll-off was applied to fill in the entire hemisphere. PAASc does not have that limitation. However, asymmetric features and the other differences discussed above aside, the comparison of the two figures does show similar aft reflection areas and similar amplitudes. The LSAF PAA data in Figure 6 have been the best available data used until the PAASc method has become available. Future refined calculations will use the 787-10 geometry for the PAASc predictions including flap deflection and other important details.

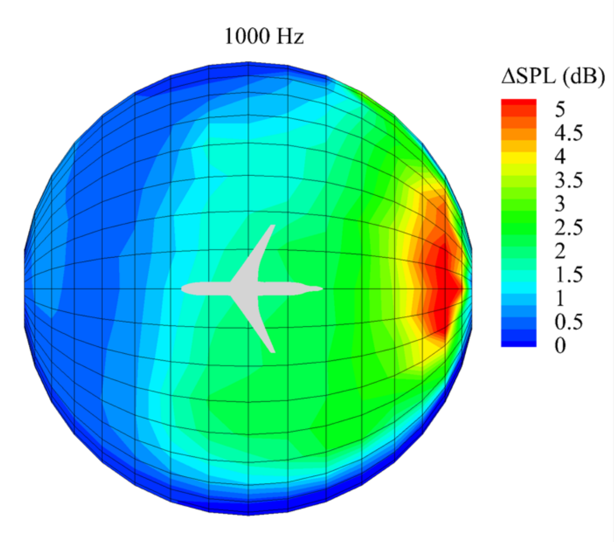

Figure 5 – PAASc-predicted scattered field of total fan broadband noise.

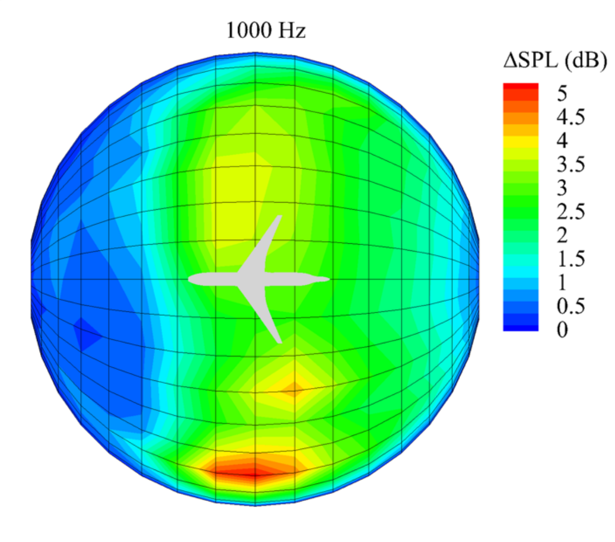

Figure 6 – Scattered field for fan broadband noise using LSAF broadband simulator data.

The flight test point shown in Figure 1 with the aircraft banking over the instrumentation was designed as a key test point for PAA effects from scattering. The engine on the same side (port) as the South Sideline microphones is at a full-power condition while the engine on the same side (starboard) as the North Sideline is at a flight idle condition. Therefore, as this test point was designed with a 34-degree bank angle, an altitude of 800 ft, and a speed of Mach 0.3, the difference between the South Sideline and the North Sideline microphones would be almost exclusively the PAA effects of the full-power engine with the South Sideline microphones primarily receiving the wing and fuselage reflected sound field and the North Sideline microphones primarily measuring the shielding and diffraction around the fuselage and wing.

In Figure 7, the measured difference between the North Sideline and the South Sideline is plotted as a function of frequency. There is close to a 10 dB difference, demonstrating the combined effects of more shielding to the North and more reflection to the South. The data are taken at a polar angle of $\theta = 90^\circ$ degrees which is directly beneath the aircraft (θ of zero corresponds to the direction of the nose with 180 degrees in the tail direction). Also shown in Figure 7 are the corresponding predictions now done at a 34-degrees bank angle to match the test condition. The dashed line is the PAASc prediction without reflection being included, meaning that the method only predicts diffraction and shielding (as the PAAShA method does). As can be seen, the method is unable to predict the reflection that is clearly focused toward the South Sideline microphones. The solid prediction line is the prediction of PAASc with reflection, diffraction, and shielding effects included in the calculation. The comparison is now excellent over a large frequency range and, together with the previous systematic validations, demonstrates that PAASc is the preferred approach for scattering PAA effects predictions.

Left to future work is the use of the 787-10 geometry instead of the generic airframe geometry used for the current predictions. While the generic geometry is sufficient for the major features of the scattering from the 787-10, the generic geometry does not have the detailed features that might have noticeable effects in the far field.

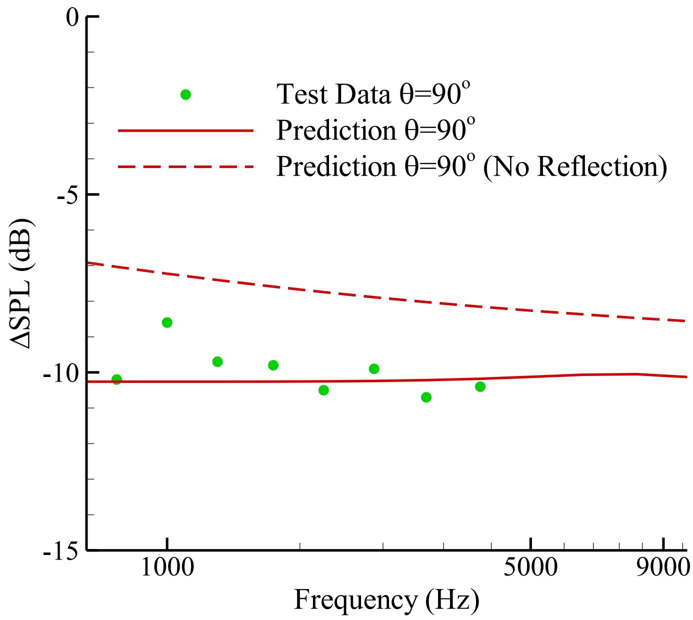

Figure 7 - Difference (measured and predicted) between the North and South Sidelines for the test point with the aircraft at 34 degrees of bank angle (800 ft altitude and Mach 0.3 speed) with one engine at full power (to the South Sideline) and the other at flight idle power (to the North Sideline). Polar angle of $\theta = 90°$.

5. Refined ANOPP-Research Predictions Compared with Flight Data

5.1 Progression of Improvements

The improvements described above may now be used to make the aircraft system level predictions, and to compare these predictions with the flight test data. Spectral results are shown first and presented as the difference between ANOPP-Research prediction and flight test data. A negative value represents underprediction relative to the measured data. For brevity and as a representative measure of the prediction accuracy, it is chosen to show results for a straight flyover of the centerline microphones with the production engine at a high power condition and the other engine at a flight idle power.

Figure 8 shows the spectral results as reported in 2022, Thomas et al. [14]. The format will be the same for the next several comparisons presented as a difference between the aircraft system level prediction and the flight test data, all at a high power engine condition and a straight flyover of the centerline microphones. Three spectra are shown corresponding to a forward angle (as the aircraft approaches the microphones), an overhead angle and an aft angle as the aircraft recedes.

In general, there was a bias to overprediction (louder than data) at low to mid frequencies with some bias to underprediction at high frequencies. In total, a range of difference with data was observed from +13 dB to -7 dB. It should be noted that for the very highest frequencies in the flight test, the roll-off prescribed by the certification rules may be used in the event the data fall below the background.

Changes to the 2022 results are applied sequentially to show the impact of each improvement more clearly. Figure 9 recomputes the aircraft system level prediction, the only change being the more accurate liner areas for the inlet and the aft ducts as discussed in section 4.1. The most noticeable change occurs in the frequencies above 3 kHz and primarily in the overhead and aft directions. This indicates that the changes in the liner areas had an impact on aft-radiated fan noise. Based on this one high power condition, the error bias is now almost entirely overprediction with a total range of +13 dB to – 2 dB.

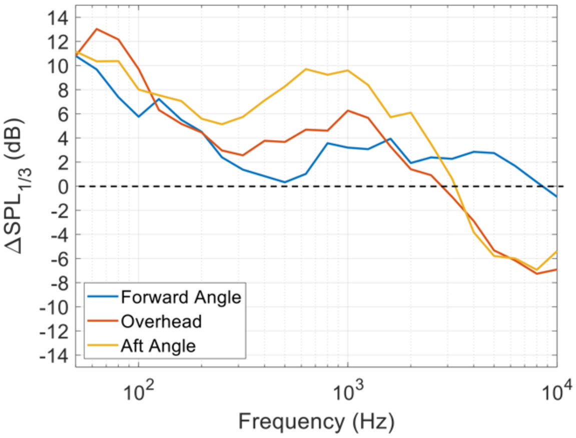

Figure 8 – 2022 reported results [14] difference of ANOPP-Research prediction minus flight data. High power condition.

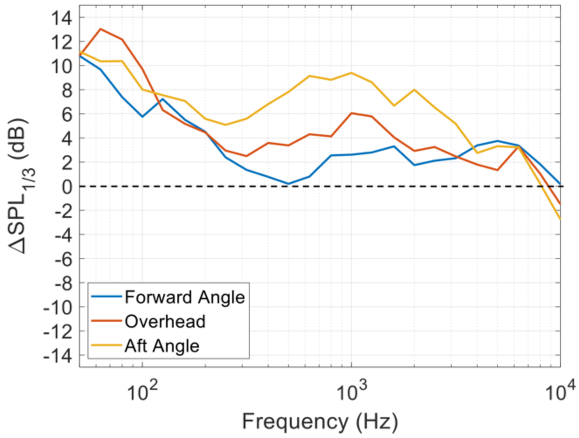

Figure 9 – Changing only the more accurate liner areas (section 4.1), ANOPP-Research prediction minus flight data. High power condition.

Figure 10 shows the application of the proposed fan source prediction method to both broadband and tones, as discussed in section 4.2, meaning there are now two changes to the 2022 predictions, the more accurate liner areas and the new proposed fan source method. As expected by the source breakdown, the proposed fan noise prediction method has greatly improved the agreement with the flight test data in the mid-to-high frequencies (400 Hz and above). The most notable improvement occurs at aft angles, where discrepancies with data at mid-frequencies are reduced from nearly 10 dB to less than 3 dB. Significant improvement is also observed at forward angles. This improvement is attributed entirely to improved inlet-radiated fan tone predictions, as the inlet-radiated fan broadband noise is still modeled using the method of Krejsa and Stone [22].

Figure 11 shows the prediction where the jet source and jet PAA effects prediction (section 4.3) have been added to the previous changes. As expected, based on the source breakdown, the improved prediction method for jet source and jet-flap interaction has greatly improved the low frequency (up to 400 Hz) accuracy at the aircraft system level when compared with the flight test data. However, the mid-frequency prediction now noticeably underpredicts the measured levels, implying that jet noise was previously predicted to be a significant contributor to mid-frequency levels at this high power setting, and that this significance is now reduced relative to fan noise.

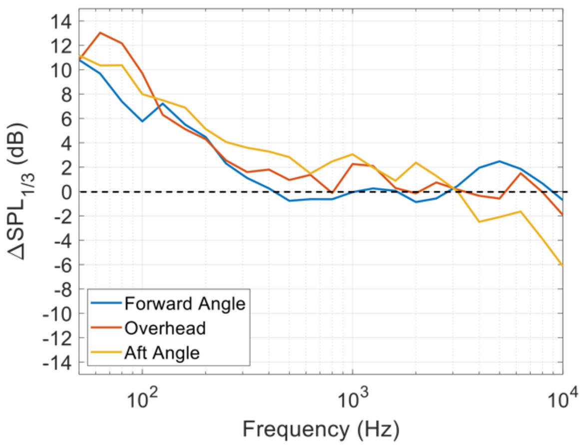

Figure 10 – Adding the proposed fan source method (section 4.2), ANOPP-Research prediction minus flight data. High power condition.

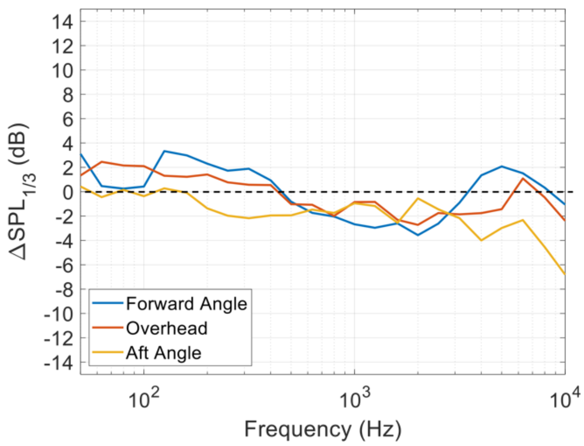

Figure 11 – Adding the jet source and jet-flap interaction PAA prediction method (section 4.3), ANOPP-Research prediction minus flight data. High power condition.

5.2 Current Refined Spectral Comparisons

In this section, the combined modifications to the ANOPP-Research prediction methodology, discussed in section 4, will be compared to the flight test data. In addition, the current comparison will be shown side-by-side with the comparison presented in 2022 [14] to directly illustrate the improvements. Figure 12 shows the comparison made in 2022 for the high power condition, with only the change being the more accurate liner areas, described in section 4.1, as these constitute more accurate inputs to the aircraft model rather than improvements in the prediction method. Note that Figure 12 is exactly the same as Figure 9 and repeated here for easier side-by-side comparison with the current improved prediction.

Figure 13 shows the prediction when, along with adding to the previous changes, the PAASc method prediction of fan broadband noise replaces the LSAF-PAA-data-based prediction. For this high power condition and spectra at three angles, the comparison of Figure 13 to Figure 11 shows that the PAASc prediction changes are mostly above 500 Hz and primarily in the overhead angle, though effects are seen at all three angles. The magnitude of the change is approximately 1 dB toward more underprediction.

The impact of the current prediction improvements can be evaluated by comparing Figures 12 and 13. Clearly there is a very significant overall improvement in two areas. First, the range of the difference over the spectra has been reduced from about 15 dB to 8 dB. Second, the prediction has gone from a strong bias toward overprediction to only a slight bias toward underprediction, particularly in the mid-frequency range (1-4 kHz) that influences EPNL most strongly. These effects combined indicate a major overall improvement in ANOPP-Research's accuracy.

To evaluate the effectiveness over the engine power line of the refined ANOPP-Research prediction capability, the spectral comparisons will be shown at a mid power and a low engine power. As before, to demonstrate progress, spectral comparisons will be shown side-by-side with the 2022 results.

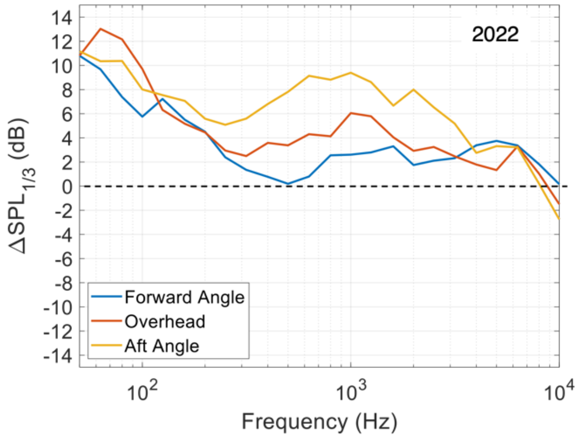

Figure 12 – Comparison of the best 2022 ANOPP-Research prediction with flight data and only adding the more accurate liner areas (section 4.1). High power condition.

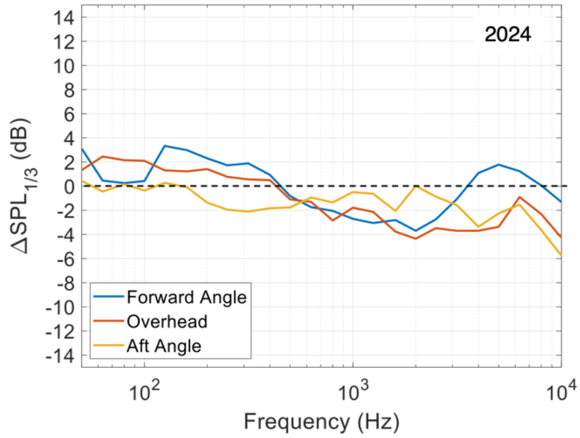

Figure 13 – Refined ANOPP-Research prediction minus flight data. All improvements (sections 4.1-4) including the PAASc fan broadband scattering prediction replacing previous LSAF-PAA-data-based method. High power condition.

Figure 14 is the result shown in 2022 at a mid power condition with only the more accurate liner areas used. Adjacent is Figure 15 with the current result for the same mid power condition and using all the improved methods described in the current work. Greater improvements in accuracy are observed at the mid power condition as compared to the high power condition.

At the low power condition, the improvement in accuracy from 2022 (Figure 16) to the current result (Figure 17) is less dramatic as compared to high and mid power conditions. However, there is still improvement as the current result is within ± 4 dB over the spectra except at the very highest frequencies, which may be most influenced by the prescribed spectral reconstruction in the measured data. Furthermore, there is also the reduction in bias as the 2022 result was almost entirely biased toward underprediction.

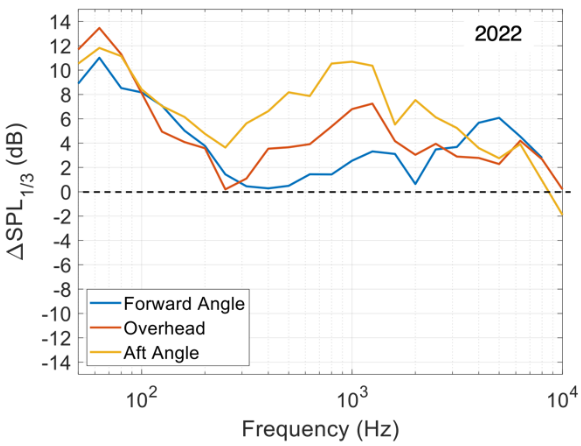

Figure 14 – Comparison of the best 2022 ANOPP-Research prediction with flight data and only adding the more accurate liner areas (section 4.1). Mid power condition.

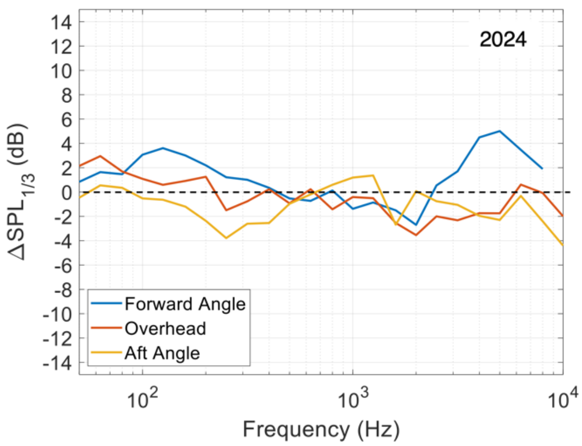

Figure 15 – Refined ANOPP-Research prediction minus flight data. All improvements (sections 4.1-4) included. Mid power condition.

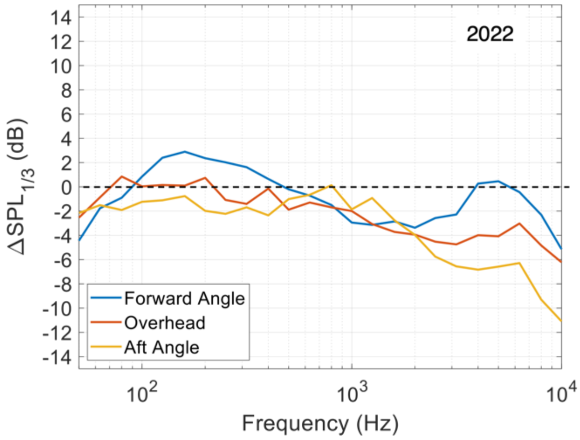

Figure 16 – Comparison of the best 2022 ANOPP-Research prediction with flight data and only adding the more accurate liner areas (section 4.1). Low power condition.

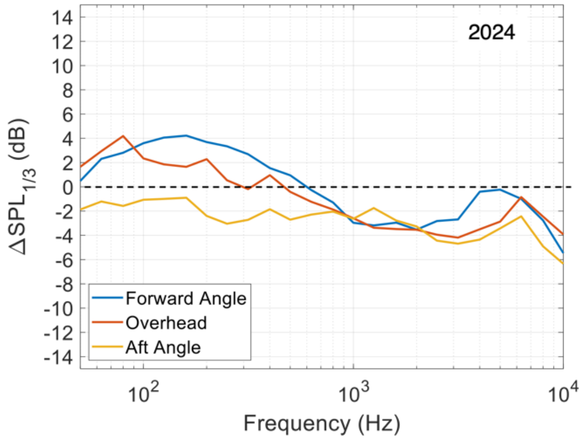

Figure 17 – Refined ANOPP-Research prediction minus flight data. All improvements (sections 4.1-4) included. Low power condition.

5.3 EPNL Comparisons

The effective perceived noise level is the metric used in noise certification as well as other evaluations. The EPNL is an integral over time and includes noy weighting and tone corrections. As such, it represents an efficient, meaningful, and single numerical value of the noise.

In the flight test, the measured data for a flyover at a test condition can be used to calculate the EPNL metric. Similarly, the prediction process for that test condition can calculate the EPNL metric. For a straight flyover at the same engine high, mid, and low power conditions used in the spectral comparisons, Table 1 shows both the measured and predicted EPNL values. Values are shown for microphones at the centerline (directly under the aircraft) as well as both sidelines (each at 1476 ft off the centerline). For the given test conditions, only one engine is at power while the other remains at flight idle resulting in an asymmetry in the total aircraft noise even for a straight flyover. This asymmetry serves as an additional measure of the fidelity to the physics of the prediction's capabilities, particularly for the PAA scattering effects which have known asymmetries. For comparison, Table 1 also shows the predicted values from 2022 with the only change to the 2022 prediction again being more accurate liner area inputs.

As seen in Table 1, The difference to data of the 2022 predictions were as much as 5.4 EPNdB with several comparisons showing 4 to 5 EPNdB differences. With the improvements described in this work, the largest difference between this 2024 prediction and flight test data is now 1.9 EPNdB, with most comparisons demonstrating much smaller differences. The accuracy holds very well over the range from low to high power, and the trends from unpowered to powered sidelines are correctly predicted. It is important to note that uncertainty in engine cycle model increases at low power settings, which may help to explain why the highest discrepancy is observed at low power. The refined ANOPP-Research predictions show progress with a difference to measured value of less than 2 EPNdB, an excellent result, especially given the statistical variability of flight test data.

Table 1 - Relative EPNdB levels of the current Refined ANOPP-Research predictions compared to measured data for three microphone linear arrays and at three engine power conditions. For reference, the 2022 initial predictions are also shown (with the more accurate liner areas). For each power condition, the measured level at the centerline is used as the reference for relative comparison.

	Low Power			Mid Power			High Power		
	Prediction		Measured	Prediction		Measured	Prediction		Measured
	2022	2024		2022	2024		2022	2024	
Unpowered Side	–12.3	–11.2	–11.7	–2.9	–8.1	–8.7	–1.9	–8.1	–7.3
Centerline	–2.6	–1.9	0.0	+4.3	+0.1	0.0	+5.0	–0.4	0.0
Powered Side	–12.0	–11.0	–10.8	–2.0	–7.9	–6.7	–0.9	–7.9	–6.2

For the high power condition, Table 1 shows the measured result of the EPNdB difference between the powered side (South Sideline) and the unpowered side (North Sideline) as 1.1 EPNdB, louder on the side of aircraft with the engine at high power. In 2022, when the fan noise PAA effects were predicted with the LSAF-PAA-data-based approach, the ANOPP-Research predicted difference between the two sidelines was 1.0 EPNdB and with the correct trend, louder on the powered side.

In this refined prediction, PAASc is now used for the EPNdB calculation to replace the LSAF-PAA-data-based approach. The result is a predicted difference between the two sidelines of 0.2 EPNdB and with the correct trend, powered to unpowered side. This is still an excellent result compared to the measured data and with reduced uncertainty of predicting to the conditions of the test point rather than using wind tunnel data as the prediction (see section 4.4 for discussion).

Together, these comparisons between the measured flight test data and the ANOPP-Research predictions, now using the PAASc physics-based prediction of PAA effects for fan broadband noise, show excellent agreement for full-scale, in-flight PAA effects of acoustic scattering as measured in the flight test.

6. Conclusions

New refined predictions have been completed and compared to the best available NASA data for subsonic transport aircraft, the Propulsion Airframe Aeroacoustics and Aircraft System Noise (PAA & ASN) Flight Research Test with a Boeing 787-10 aircraft. The refinements proposed are to the system noise prediction capability of NASA, ANOPP-Research, and include:

- More accurate inputs for the inlet and aft duct liner areas,
- A proposed fan source noise prediction method for both broadband and tones,
- A model scale data-based prediction of jet source noise with the pylon effect and of the jet-flap interaction,
- An acoustic scattering prediction method, PAASc, used to predict the scattering of fan broadband noise.

The combination of the improved methods were evaluated by comparing to the PAA & ASN Boeing 787-10 flight test data. The comparisons of ANOPP-Research predictions and flight test data are summarized as:

- Over the power range of the engine, differences are typically within ± 4 dB over the whole spectral range,
- The prediction is not strongly biased toward either over or underprediction, again, over the whole engine power range, and
- On an EPNdB level, the predictions are within 2 EPNdB for centerline microphones directly underneath the aircraft flyover and on both sidelines even with an asymmetrical aircraft noise source where one engine is at power and the other at flight idle.

These high level results represent a significant improvement over the initial predictions reported in 2022 and are the result of prediction method development in the following areas:

- The PAASc method for acoustics scattering has been extensively validated with a wide variety of lab, wind tunnel, and now flight test data. Additional improvements are possible to extend its applicability. It is important to note that PAASc meets the system noise requirements for fully 3D geometries with complex features and yet has extremely fast run times on the order of minutes for full scale aircraft, well within the range required for a versatile and effective design capability.
- The proposed fan source noise method for broadband and tones has shown a major improvement over the previous best NASA method and met an area of high priority need given the importance of fan source noise. The proposed method will be used while it is being extended to the inlet and formalized as a new method in ANOPP.
- The data-based predictions of jet source with pylon effect and jet-flap interaction are expected to be developed into more general prediction methods.

These improved prediction capabilities and others under development at NASA, represent a major advancement in NASA's ability to accurately predict the acoustics of subsonic transport aircraft for a variety of conditions, technologies, and flight operations. As the methods are thoroughly tested and formalized, these methods are intended to be released in ANOPP for US users.

A new duct liner attenuation method remains a top priority for the necessary capability to predict the impact of different liner technologies as well as more realistic features such as bifurcation liners, for example.

The Propulsion Airframe Aeroacoustics and Aircraft System Noise (PAA & ASN) Flight Research Test data with the Boeing 787-10 will continue to be the standard to measure prediction accuracy. In the short term, predictions are planned to be improved in several ways mentioned throughout the paper.

7. Acknowledgments

The extraordinary support and funding of this research, for both the flight test and the analysis, by the NASA Advanced Air Transport Technology Project is gratefully acknowledged. The exceptional efforts of The Boeing Company and the Boeing ecoDemonstrator Program are gratefully acknowledged in the execution of this challenging flight test under difficult circumstances in the summer of 2020.

8. Contact Author Email Address

For more information, please contact the lead author, Russell.H.Thomas@NASA.gov

9. Copyright Statement

References

[1] Thomas, R.H., Burley, C.L., and Olson, E.D., "Hybrid Wing Body Aircraft System Noise Assessment with Propulsion Airframe Aeroacoustic Experiments," *International Journal of Aeroacoustics*, Vol. 11 (3+4), pp. 369-410, 2012. doi:10.1260/1475-472X.11.3-4.369

[2] Guo, Y. and Thomas, R.H., "System Noise Assessment of Hybrid Wing-Body Aircraft with Open-Rotor Propulsion," *AIAA Journal of Aircraft*, Vol. 52, No. 6, 2015, pp. 1767-1779. doi:10.2514/1.C033048

[3] Thomas, R.H., Burley, C.L., Lopes, L.V., Bahr, C.J., Gern, F.H., and Van Zante, D.E., "System Noise Assessment and the Potential for a Low Noise Hybrid Wing Body Aircraft with Open Rotor Propulsion," AIAA Paper 2014-0258, 52nd AIAA Aerospace Sciences Meeting, National Harbor, Maryland, January 13-17, 2014. doi:10.2514/6.2014-0258

[4] Thomas, R.H., Burley, C.L., and Nickol, C.L., "Assessment of the Noise Reduction Potential of Advanced Subsonic Transport Concepts for NASA's Environmentally Responsible Aviation Project," AIAA Paper 2016-0863, 54th AIAA Aerospace Sciences Meeting, San Diego, California, January 4-8, 2016. doi:10.2514/6.2016-0863

[5] Thomas, R.H., Guo, Y., Berton, J.J., and Fernandez, H., "Aircraft Noise Reduction Technology Roadmap Toward Achieving the NASA 2035 Noise Goal," AIAA Paper 2017-3193, 23rd AIAA/CEAS Aeroacoustics Conference, Denver, Colorado, June 5-9, 2017. doi:10.2514/6.2017-3193

[6] Guo, Y., Thomas, R.H., Clark, I.A., and June, J.C., "Far-Term Noise Reduction Roadmap for the Midfuselage Nacelle Subsonic Transport," *AIAA Journal of Aircraft*, Vol. 56, No. 5, 2019, pp. 1893–1906. doi:10.2514/1.C035307

[7] Clark, I.A., Thomas, R.H., and Guo, Y., "Aircraft System Noise of the NASA D8 Subsonic Transport Concept," *AIAA Journal of Aircraft*, Vol. 58, No. 5 (2021), pp. 1106-1120. doi:10.2514/1.C036259

[8] June, J.C., Thomas, R.H., Guo, Y., and Clark, I.A., "Far Term Noise Reduction Technology Roadmap for a Large Twin-Aisle Tube-and-Wing Subsonic Transport," AIAA Paper 2019-2428, 25th AIAA/CEAS Aeroacoustics Conference, Delft, The Netherlands, May 20-23, 2019. doi:10.2514/6.2019-2428

[9] June, J.C., Thomas, R.H., and Guo, Y., "System Noise Reduction Roadmaps for both a Transonic Truss-Braced Wing and a Peer Conventional Configuration," AIAA Paper 2022-3049, 28th AIAA/CEAS Aeroacoustics Conference, Southampton, UK, June 14-17, 2022. doi:10.2514/6.2022-3049

[10] Shelts, K.M., Clark, I.A., and Thomas, R.H., "Aircraft System Noise Assessment of the NASA Single-Aisle Over-the-Wing Nacelle Configuration," AIAA 2022-3048, 28th AIAA/CEAS Aeroacoustics Conference, Southampton, UK, June 14-17, 2022. doi:10.2514/6.2022-3048

[11] Hubbard, H. (editor), "Aeroacoustics of Flight Vehicles: Theory and Practice, Volume 1: Noise Sources," NASA Reference Publication 1258, August,1991. URL:https://ntrs.nasa.gov/citations/19920001380

[12] Hubbard, H. (editor), "Aeroacoustics of Flight Vehicles: Theory and Practice, Volume 2: Noise Control," NASA Reference Publication 1258, August 1991. URL:https://ntrs.nasa.gov/citations/19920005561

[13] Dahl. M. (editor), "Assessment of NASA's Aircraft Noise Prediction Capability," NASA TP 2012-215653, July 2012. URL:https://ntrs.nasa.gov/citations/20120012957

[14] Thomas, R.H., Guo, Y., Clark, I.A., and June, J.C., "Propulsion Airframe Aeroacoustics and Aircraft System Noise Flight Research Test: NASA Overview," AIAA Paper 2022-2993, 28th AIAA/CEAS Aeroacoustics Conference, Southampton, UK, June 14-17, 2022. doi:10.2514/6.2022-2993

[15] Czech, M.J., Thomas, R.H., Guo, Y., June, J.C., Clark, I.A., and Shoemaker, C.M., "Propulsion Airframe Aeroacoustics and Aircraft System Noise Flight Test on the ecoDemonstrator 2020 – Boeing 787 Testbed Aircraft," AIAA Paper 2022-2994, 28th AIAA/CEAS Aeroacoustics Conference, Southampton, UK, June 14-17, 2022. doi:10.2514/6.2022-2994

[16] Guo, Y. and Thomas, R.H., "Assessment of Next Generation Airframe System Noise Prediction Methods with PAA and ASN Flight Test Data," AIAA Paper 2022-2995, 28th AIAA/CEAS Aeroacoustics Conference, Southampton, UK, June 14-17, 2022. doi:10.2514/6.2022-2995

[17] Clark, I.A., Thomas, R.H., and Guo, Y., "Fan Acoustic Flight Effects on the PAA & ASN Flight Test," AIAA Paper 2022-2996, 28th AIAA/CEAS Aeroacoustics Conference, Southampton, UK, June 14-17, 2022. doi:10.2514/6.2022-2996

[18] Raney, J.P., Padula, S.L., and Zorumski, W.E., "NASA Progress in Aircraft Noise Prediction," NASA Technical Memorandum 81915, March 1981. URL:https://ntrs.nasa.gov/citations/19810012301

[19] Zorumski, William E., "Aircraft Noise Prediction Program Theoretical Manual," NASA Technical Memorandum 83199, February 1982. URL:https://ntrs.nasa.gov/citations/19820012072

[20] Lopes, L.V. and Burley, C.L., "ANOPP2's User Manual," Tech. Rep. NASA/TM-2016-219342, October 2016. URL:https://ntrs.nasa.gov/citations/20160014858

[21] Kontos, K.B., Kraft, R.E., and Gliebe, P.R., "Improved NASA-ANOPP Noise Prediction Computer Code for Advanced Subsonic Propulsion Systems, Volume 2: Fan Suppression Model Development," Tech. Rep. CR-202309, NASA, December 1996. URL:https://ntrs.nasa.gov/citations/19970005047

[22] Krejsa, E.A. and Stone, J.R., "Enhanced Fan Noise Modeling for Turbofan Engines," NASA CR-2014-218421, December 2014. URL:https://ntrs.nasa.gov/citations/20150000884

[23] Herkes, W. H., Olsen, R. F., and Uellenberg, S., "The Quiet Technology Demonstrator Program: Flight Validation of Airplane Noise-Reduction Concepts," AIAA Paper 2006-2720, 12th AIAA/CEAS Aeroacoustics Conference, Cambridge, Massachusetts, May 8-10, 2006. doi:10.2514/6.2006-2720

[24] Clark, I.A., Nesbitt, E.H., Thomas, R.H., and Guo, Y., "Turbofan Aft-Radiated Broadband Acoustic Flight Effects," AIAA Paper 2024-3225, 30th AIAA/CEAS Aeroacoustics Conference, Rome, Italy, June 4-7, 2024. doi:10.2514/6.2024-3225

[25] Nesbitt, E., Clark, I.A., Guo, Y., and Thomas, R.H., "Flight Effects on Turbofan Fan Tones," AIAA Paper 2024-3222, 30th AIAA/CEAS Aeroacoustics Conference, Rome, Italy, June 4-7, 2024. doi:10.2514/6.2024-3222

[26] Stone, J.R., Krejsa, E.A., Clark, B.J., and Berton, J.J., "Jet Noise Modeling for Suppressed and Unsuppressed Aircraft in Simulated Flight," Tech. Rep., NASA TM-2009-215524, March 2009. URL: https://ntrs.nasa.gov/citations/20090015381

[27] Czech, M.J., Thomas, R.H., and Elkoby, R., "Propulsion Airframe Aeroacoustic Integration Effects for a Hybrid Wing Body Aircraft Configuration," *International Journal of Aeroacoustics*, Vol. 11 (3+4), pp. 335-368, 2012. doi:10.1260/1475-472X.11.3-4.335

[28] Thomas, R.H., Czech, M.J., and Doty, M.J., "High Bypass Ratio Jet Noise Reduction and Installation Effects Including Shielding Effectiveness," AIAA Paper 2013-0541, 51st AIAA Aerospace Sciences Meeting, Grapevine, Texas, January 7-10, 2013. doi:10.2514/6.2013-541

[29] Czech, M.J. and Thomas, R.H., "Open Rotor Aeroacoustic Installation Effects for Conventional and Unconventional Airframes," AIAA Paper 2013-2185, 19th AIAA/CEAS Aeroacoustics Conference, Berlin, Germany, May 27-29, 2013. doi:10.2514/6.2013-2185

[30] Mengle, V.G., Elkoby, R., Brusniak, L., and Thomas, R.H., "Reducing Propulsion Airframe Aeroacoustic Interactions with Uniquely Tailored Chevrons: 1. Isolated Nozzles," AIAA Paper 2006-2467, 12th AIAA/CEAS Aeroacoustics Conference, Cambridge, Massachusetts, May 8-10, 2006. doi:10.2514/6.2006-2467

[31] Mengle, V.G., Elkoby, R., Brusniak, L., and Thomas, R.H., "Reducing Propulsion Airframe Aeroacoustic Interactions with Uniquely Tailored Chevrons: 2. Installed Nozzles," AIAA Paper 2006-2434, 12th AIAA/CEAS Aeroacoustics Conference, Cambridge, Massachusetts, May 8-10, 2006. doi:10.2514/6.2006-2434

[32] Mengle, V.G., Elkoby, R., Brusniak, L., and Thomas, R.H., "Reducing Propulsion Airframe Aeroacoustic Interactions with Uniquely Tailored Chevrons: 3. Jet-Flap Interaction," AIAA Paper 2006-2435, 12th AIAA/CEAS Aeroacoustics Conference, Cambridge, Massachusetts, May 8-10, 2006. doi:10.2514/6.2006-2435

[33] Viswanathan, K. and Lee, I.C., "Investigations of Azimuthal and Flight Effects on Noise from Realistic Turbofan Exhaust Geometries," *AIAA Journal*, Vol. 51, No. 6, 2013, pp. 1486-1505. doi: 10.2514/1.J052138

[34] Thomas, R.H. and Guo, Y., "Systematic Validation of the PAAShA Shielding Prediction Method," *International Journal of Aeroacoustics* 2022*,* Vol. 21(5-7), pp. 558-584. doi: 10.1177/1475472X221107369

[35] Guo, Y. and Thomas, R.H., "Geometric Acoustics for Aircraft Noise Scattering," AIAA Paper 2022-3077, 28th AIAA/CEAS Aeroacoustics Conference, Southampton, UK, June 14-17, 2022. doi:10.2514/6.2022-3077